Editors' Suggestion

Effect of applied orthorhombic lattice distortion on the antiferromagnetic phase of $CeAuSb_2$

Joonbum Park,[1,2] Hideaki Sakai,[3,4] Onur Erten,[5] Andrew P. Mackenzie,[1,6,*] and Clifford W. Hicks[1,†]

[1]*Max Planck Institute for Chemical Physics of Solids, Nöthnitzer Straße 40, 01187 Dresden, Germany*

[2]*Max Planck POSTECH Center for Complex Phase Materials, Pohang University of Science and Technology, Pohang 37673, Republic of Korea*

[3]*Department of Physics, Osaka University, Toyonaka, Osaka 560-0043, Japan*

[4]*PRESTO, Japan Science and Technology Agency, Kawaguchi, Saitama 332-0012, Japan*

[5]*Max Planck Institute for the Physics of Complex Systems, Nöthnitzer Straße 38, 01187 Dresden, Germany*

[6]*Scottish Universities Physics Alliance, School of Physics and Astronomy, University of St. Andrews, St. Andrews KY16 9SS, United Kingdom*

(Received 25 August 2017; revised manuscript received 26 October 2017; published 11 January 2018)

We study the response of the antiferromagnetism of $CeAuSb_2$ to orthorhombic lattice distortion applied through in-plane uniaxial pressure. The response to pressure applied along a ⟨110⟩ lattice direction shows a first-order transition at zero pressure, which shows that the magnetic order spontaneously lifts the $(110)/(1\bar{1}0)$ symmetry of the unstressed lattice. Sufficient ⟨100⟩ pressure appears to rotate the principal axes of the order from ⟨110⟩ to ⟨100⟩. At low ⟨100⟩ pressure, the transition at T_N is weakly first order; however, it becomes continuous above a threshold ⟨100⟩ pressure. We discuss the possibility that this behavior is driven by order parameter fluctuations, with the restoration of a continuous transition being a result of reducing the point-group symmetry of the lattice.

DOI: 10.1103/PhysRevB.97.024411

I. INTRODUCTION

Transitions in condensed-matter systems are defined by their broken symmetries. Electronic orders can sometimes lift the point-group symmetry of their host lattices, for example, twofold rotationally symmetric order on a tetragonal lattice. This is an intriguing possibility in part because fluctuations can have nontrivial effects on such transitions [1]. Condensation of a particular order can also obscure strong subleading susceptibilities to alternative orders, which one wants to know about to construct a good theory of the processes driving phase formation [2]. As we present in this article, uniaxial pressure can be used to probe both of these possibilities.

We study the heavy-fermion antiferromagnet $CeAuSb_2$, a layered, tetragonal compound with Néel temperature $T_N = 6.5$ K [3,4]. We found in-plane uniaxial pressure to have a strong effect on the magnetic transition, in ways more pertinent to general questions of how magnetic order and lattice symmetry interact than specifically to heavy-fermion physics. An important aspect of our work is that the pressure is applied using piezoelectric actuators, allowing *in situ* tunability. For example, upon ramping the pressure at constant temperature a first-order transition, with hysteresis, is observed at zero pressure. This transition's existence proves that the magnetic order lifts the point-group symmetry of the lattice. We also probe a long-standing prediction that a transition driven first-order by fluctuations should become continuous when uniaxial pressure selects a preferred direction [5,6], with much higher resolution than before. Finally, there is no requirement to apply high pressures at room temperature, where samples are more susceptible to plastic deformation than at low temperature.

All measurements here were done in zero magnetic field. Our samples were grown by a self-flux method [7,8] and have residual resistivity ratios (RRRs) $R(300\,\mathrm{K})/R(1.5\,\mathrm{K})$ between 6 and 9. A shoulder in the resistivity $\rho(T)$ of $CeAuSb_2$ marks the Kondo temperature, $T_K \sim 14$ K [9]. Therefore, at T_N the cerium moments should be incorporated into the Fermi sea, and there is thermodynamic evidence that they are: The heat capacity has a Fermi liquid form (i.e., proportional to T) between T_N and ∼10 K, and below T_N shows good entropy balance with a Fermi liquid [10]. Recent neutron scattering data suggest that the magnetic order itself is itinerant [11]: It was found to be an incommensurate spin-density wave polarized along the c axis, meaning that the polarization must vary from site to site, which is not generally expected for local-moment order. The propagation vector is $(\eta,\eta,1/2)$, with η varying between 0.130 and 0.136 depending on field and field history.

Our apparatus is described in Ref. [12]. Briefly, samples are prepared as beams with high length-to-thickness and length-to-width aspect ratios, and their ends are held in the apparatus with epoxy, allowing application of both compressive and tensile stresses along their length. A photograph of a mounted sample is shown in Fig. 1(a). The sample is under conditions of uniaxial stress: The stress is nonzero along the long axis of the sample and zero along transverse directions. However, because the apparatus has a high spring constant relative to that of typical samples, the applied displacement is the more directly controlled variable than the applied force. For samples such as $CeAuSb_2$, whose elastic moduli have not been reported, we may estimate the applied strain but do not know the stress. The displacement applied to the sample and sample-mounting epoxy is measured with a capacitive displacement sensor, and

*mackenzie@cpfs.mpg.de
†hicks@cpfs.mpg.de

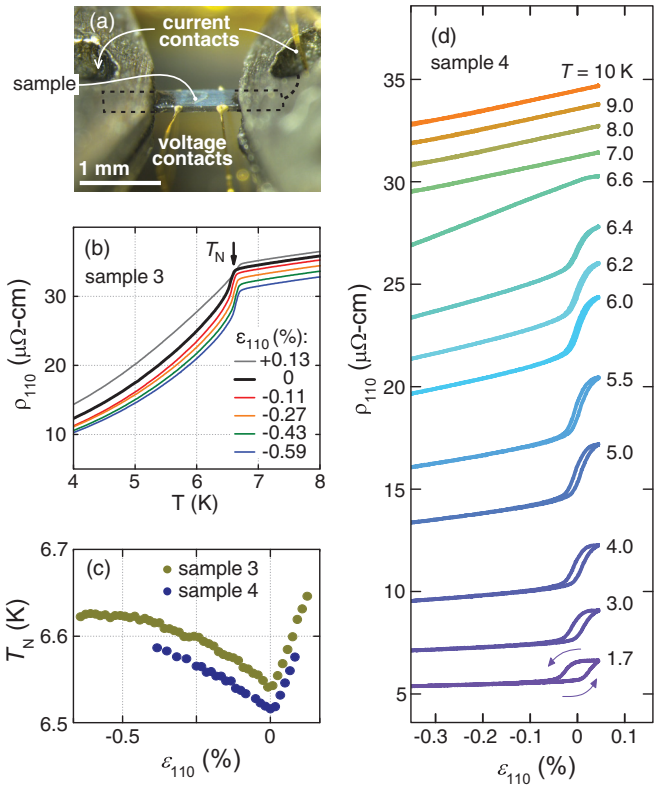

FIG. 1. Results for ⟨110⟩ pressure. (a) Photograph of a mounted sample. (b) Resistivity $\rho_{110}(T)$ along a ⟨110⟩ lattice direction at various fixed strains ε_{110}. (c) Néel temperature $T_N(\varepsilon_{110})$, identified at each strain as the maximum in $d\rho_{110}/dT$. (d) $\rho_{110}(\varepsilon_{110})$ at various fixed temperatures. Arrows indicate the direction of the strain ramp. In (b)–(d), $\varepsilon_{110} = 0$ is set to the location of the cusps in $T_N(\varepsilon_{110})$, seen in (c).

the strain in the sample is estimated as this displacement times 0.8 divided by the exposed length of the sample. The factor of 0.8 is an estimate for the effects of elastic deformation of the epoxy, which allows some relaxation of the sample strain [12,13].

We measure the resistivity, which is strongly affected by the magnetic order [3,4], along the length of the samples. The strain-induced change in sample resistance has a geometric contribution due to the applied change in sample dimensions, typically of magnitude $\Delta R/R \sim 2\varepsilon$, where ΔR is the change in resistance and ε is the applied strain [14]. We find R to vary much more strongly with strain than this and so neglect this geometric effect in all plots and analysis below.

II. RESULTS: ⟨110⟩ PRESSURE

Five samples were measured under pressure, three cut along a ⟨100⟩ lattice direction (that is, along the Ce-Ce bond direction) and two along a ⟨110⟩ direction. Results for ⟨110⟩ pressure (inducing longitudinal strain ε_{110}) are presented in Figs. 1(b) through 1(d). Figure 1(b) shows resistivity versus temperature at various applied strains. The Néel transition is clearly seen in each curve, and an immediately apparent result is that the quantitative effect of ⟨110⟩ pressure on T_N is small: Compression by 0.6% shifts T_N by only ∼0.1 K.

However, when T_N is plotted against ε_{110}, in Fig. 1(c), a sharp cusp in $T_N(\varepsilon_{110})$ becomes apparent. If the cusp is at $\varepsilon_{110} = 0$, it indicates a two-component order parameter, in which each component lifts the $(110)/(1\bar{1}0)$ symmetry of the lattice. Under this hypothesis, ⟨110⟩ pressure favors one of these components, and the favored component switches when the sign of the pressure changes, yielding the sharp change in slope $dT_N/d\varepsilon_{110}$. It is a reasonable hypothesis that the cusp marks $\varepsilon_{110} = 0$. First, the strain applied to reach the cusp, ∼0.1%, is compatible with plausible differential thermal contractions between the sample and apparatus frame (which is made of titanium). Second, samples fractured when tensioned by more than ∼0.2% beyond the cusp, so at that point they were definitely under tension.

If the two components coexist microscopically over some strain range, strain ramps below T_N should show two transitions, corresponding separately to the onset of one and the disappearance of the other component [15]. If they do not coexist, the ordered state spontaneously lifts the $(110)/(1\bar{1}0)$ symmetry of the lattice, and a first-order transition, corresponding to reversal of the sign of the symmetry breaking, is expected at $\varepsilon_{110} = 0$. Our results, shown in Fig. 1(d), show a first-order transition: $\rho(\varepsilon_{110})$ changes in a steplike manner, and there is clear hysteresis. Within our resolution, it extends up to T_N. The neutron data also point to spontaneous symmetry breaking: the observed scattering peaks correspond to incommensurate spin-density-wave propagation vectors $\mathbf{q} = (\eta, \eta, 1/2)$ and $(\eta, -\eta, 1/2)$, and the absence of peaks corresponding to mixing of these components indicates that they exist in separate domains [11]. Therefore, we conclude firmly that the magnetic order spontaneously lifts the $(110)/(1\bar{1}0)$ symmetry of the lattice and assign the location of the cusp as $\varepsilon_{110} = 0$.

The cusp in $T_N(\varepsilon_{110})$ is not symmetric: $|dT_N/d\varepsilon_{110}|$ is smaller on the compressive than on the tension side of the cusp. This is not surprising: Uniaxial pressure applies not only an in-plane orthorhombicity, i.e., a nonzero $\varepsilon_{110} - \varepsilon_{1\bar{1}0}$, but also changes to unit-cell volume and c-axis lattice parameter. Coupling to the latter two variables will introduce such asymmetry.

Another feature apparent in the data above, also noted in Ref. [9] and which will be important in discussing results of ⟨100⟩ pressure, is that the transition at T_N appears to be weakly first order. Although we did not resolve hysteresis between increasing- and decreasing-temperature ramps, there is a clear step in $\rho(\varepsilon_{110})$ at T_N. For further evidence, the heat capacity of an unstrained crystal was measured, with the results shown in Fig. 2. The sharp peak in heat capacity at T_N strongly suggests a first-order transition.

III. RESULTS: ⟨100⟩ PRESSURE

We now turn to results from ⟨100⟩ pressure. As described in the Introduction, there is strong evidence that the magnetic order of $CeAuSb_2$ is an itinerant order, with the Ce magnetic moments incorporated into the Fermi sea through the Kondo effect at a temperature well above T_N. The Kondo temperature of $CeAuSb_2$ has been shown to be tunable with hydrostatic pressure [9]: It increases by a factor of ∼2 under 2 GPa.

We find that uniaxial pressure has a much smaller effect on the Kondo temperature. In Fig. 3 we show the longitudinal resistivity of a sample cut along a ⟨100⟩ crystal direction at a

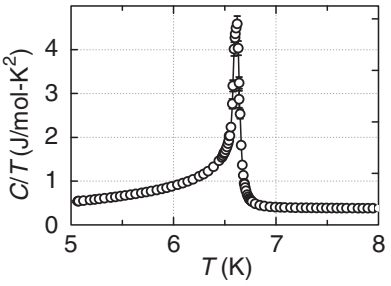

FIG. 2. Heat capacity of an unpressurized crystal of $CeAuSb_2$, with a mass of 2.2 mg. The sharp peak is consistent with a first-order transition.

few applied strains ε_{100}. The shoulder at ∼14 K indicates the Kondo temperature and is at constant temperature to within 1 K over the range of strains studied. Similarly, T_K of $CeRu_2Si_2$ was also found to have a very weak dependence on in-plane uniaxial pressure [16]. Therefore, over the range of ⟨100⟩ strains studied in this paper, we may safely assume that T_K remains well above T_N and that we are probing an itinerant magnetic order.

$\rho(T)$ at various applied strains for one sample is shown in Fig. 4. To make more clear the first-order-like nature of the transition at low strains, the derivative $d\rho/dT$ is plotted in the lower panel. In the response to ⟨100⟩ pressure there is no obvious feature that might be identified with zero strain, so we take zero strain to be at the same applied displacement where the cusp in $T_N(\varepsilon_{110})$ was observed. Variability in the precise mounting conditions achieved will introduce an error of ∼0.1% on this determination.

Strains $|\varepsilon_{100}| < 0.25\%$ do not strongly affect the transition; over this range, compression weakly suppresses T_N and possibly reduces the size of the first-order-like jump in ρ. However, at higher compression, $\varepsilon_{100} < -0.25\%$, the first-order jump disappears, and the transition splits into two features. The upper feature is a downturn in the slope $d\rho/dT$, and the lower feature is a further downturn; we label their temperatures T_2 and T_1. We hypothesize that an equivalent splitting would occur under tensile strain; in the data in Fig. 4, the first-order jump also shrinks somewhat under tensile pressure. However, attempts to reach this hypothesized splitting in samples 1 and 2 resulted

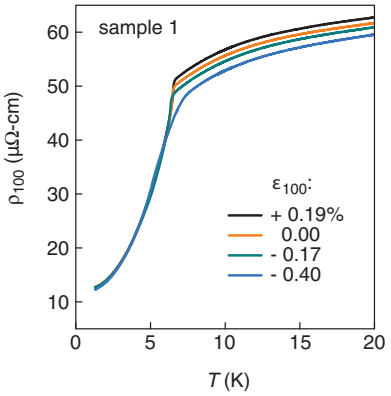

FIG. 3. Longitudinal resistivity $\rho_{100}(T)$ for sample 1 and various fixed ε_{100}. The shoulder at ∼14 K marks the Kondo temperature, which is not strongly affected by strain.

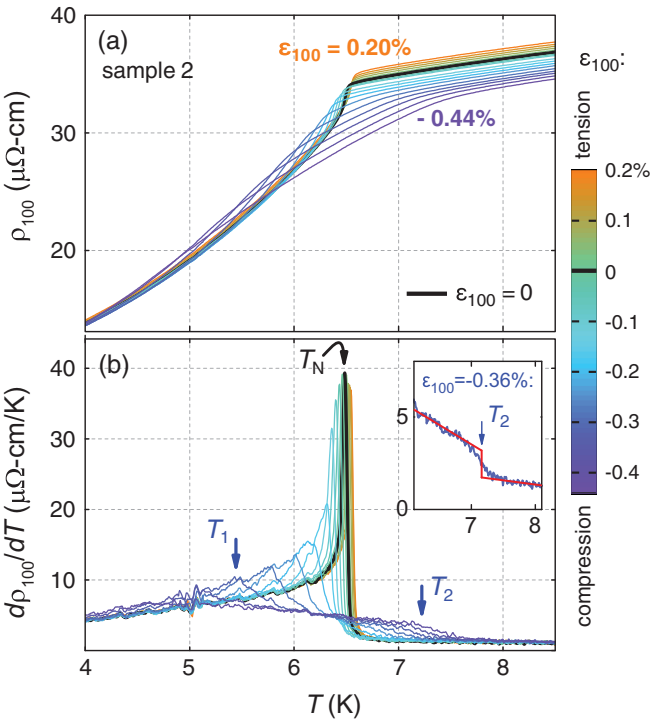

FIG. 4. Results from ⟨100⟩ pressure. (a) Resistivity $\rho_{100}(T)$ along a ⟨100⟩ lattice direction at various fixed strains ε_{100} and (b) the corresponding derivatives $d\rho_{100}/dT$. The temperature T_1 is identified as the peak in $d\rho/dT$, and T_2 is identified as the step in $d\rho/dT$.

in both samples fracturing. The samples broke at a sufficiently low strain, $\varepsilon_{100} \sim +0.25\%$, that an essentially symmetric strain response is not ruled out.

In Fig. 5 we plot ρ_{100} against ε_{100} at fixed temperatures. The feature at T_2 is visible as a change in slope $d\rho/d\varepsilon$ in the 7.0 to 8.5 K curves. We assign this feature to be a second-order transition: The slopes $d\rho/d\varepsilon$ and $d\rho/dT$ both change, but no first-order steps in ρ are apparent.

The feature at T_1 is visible in, for example, the 6.0 K curve as a peak in ρ_{100} at $\varepsilon_{100} \sim -0.3\%$. As the temperature is reduced, it moves towards higher compressions and changes from a peak into a steplike feature. It is suppressed to below 2 K at $\varepsilon_{100} \sim -0.5\%$. The steplike form at lower temperatures suggests a first-order transition. For further evidence we performed strain ramps at constant temperature, with the results shown in Fig. 5(b). Small hysteresis loops are resolvable at temperatures below ∼4 K.

We also probe the transverse resistance by running current and measuring voltage across the width of the sample, as illustrated in Fig. 5(c). In this configuration the current flow is not homogeneous, so we do not attempt to extract a quantitatively precise transverse resistivity. However, the data reveal, as shown in Fig. 5(c), that the transverse resistivity changes opposite to the longitudinal resistivity across the transition at $\varepsilon_{100} \approx -0.5\%$. Also, the transverse resistivity changes in a sharp, first-order step. We show in Fig. 6 the transverse resistivity at 1.5 K measured in increasing- and decreasing-strain ramps, which reveal observable hysteresis: It is a first-order transition. Generically, the change in longitudinal resistivity should be as sharp as the change in transverse resistivity,

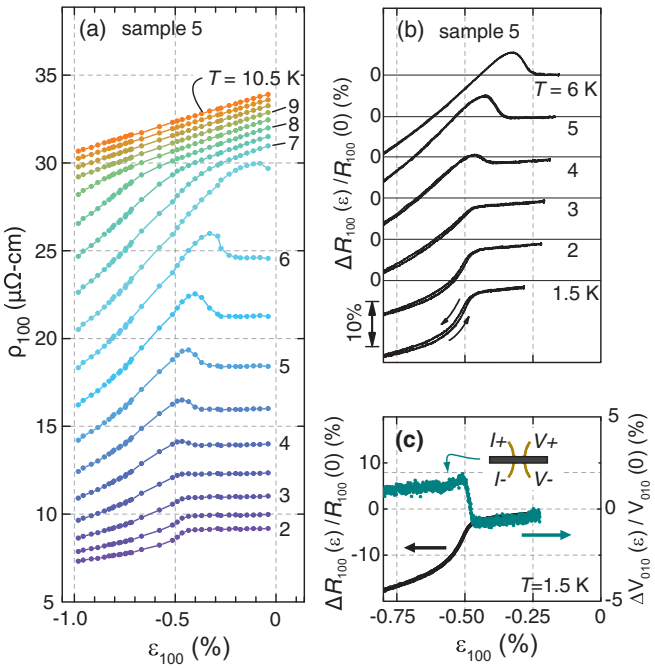

FIG. 5. (a) $\rho_{100}(\varepsilon_{100})$ at fixed temperatures on a 0.5 K interval. The data were collected in temperature ramps. (b) Change in resistance $\Delta R_{100}/R_{100}(\varepsilon_{100}=0)$ during increasing- and decreasing-strain ramps at fixed temperatures. There is hysteresis below ~4 K. (c) For a qualitative measure of the transverse resistivity ρ_{010}, current was applied across the width of one sample, as indicated in the diagram of the contact configuration. The resulting voltage across the sample V_{010} is plotted, along with the longitudinal resistance.

and a possible reason that in the data it is not is that the transverse configuration probes, effectively, a smaller volume of the sample.

The first-order transition does not appear to extend up to T_N. The hysteresis disappears, and the form of $\rho(\varepsilon_{100})$ changes from steplike to peaked at $T \sim 3.5$ K. The peaked form of $\rho(\varepsilon_{100})$ at higher temperatures may be a result of critical fluctuations above the end point of the first-order transition.

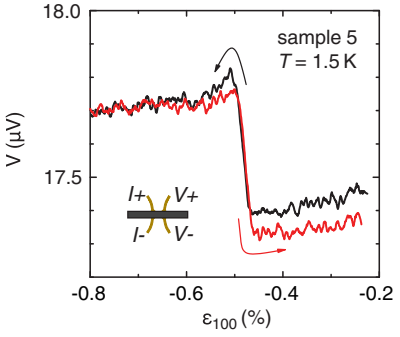

FIG. 6. Transverse response of the sample across the transition at $\varepsilon_{100} \approx -0.5\%$, from increasing- and decreasing-strain ramps. The hysteresis shows that the transition is first-order.

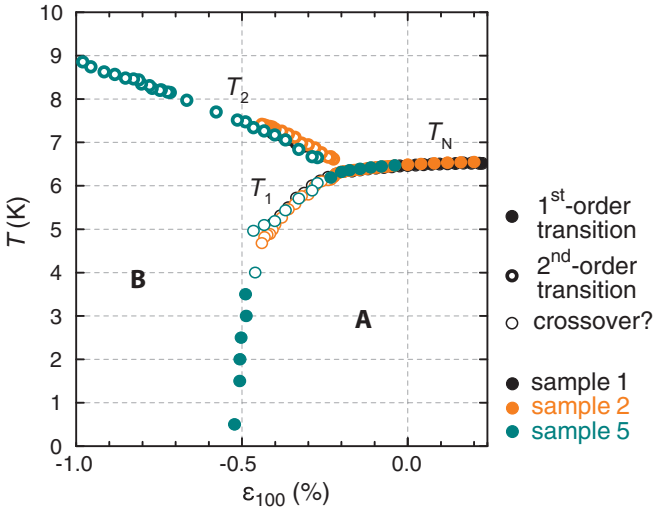

FIG. 7. (a) T-ε_{100} phase diagram. T_N is taken as the maximum in $d\rho/dT$. T_2 is taken as the midpoint of the step in $d\rho/dT$, as shown in Fig. 4(b). T_1 is taken at higher temperatures as the peak in $d\rho/dT$ [see Fig. 4(b)] and at lower temperatures as the approximate midpoint of the step in $\rho(\varepsilon_{100})$ [see Fig. 5(a)]. The in-plane propagation vector is $(\eta, \pm\eta)$ for phase A, and we propose that it is $(\eta_2,0)$ or $(0,\eta_2)$ for phase B.

IV. DISCUSSION AND CONCLUSION

As explained above, we conclude, in agreement with neutron data [11], that the magnetic order of unstressed $CeAuSb_2$ spontaneously lifts the $(110)/(1\bar{1}0)$ symmetry of the lattice. The V-shaped form of $T_N(\varepsilon_{110})$ indicates two anisotropic order parameter components, with $\langle 110\rangle$ principal axes, and the first-order transition across ε_{110} shows that they do not coexist microscopically. We note that $Sr_3Ru_2O_7$ provides an alternative example of anisotropic order parameter components, and in that material they do coexist microscopically over a nonzero range of applied lattice orthorhombicity [15].

However, although the spontaneous symmetry breaking is with $\langle 110\rangle$ principal axes, $\langle 100\rangle$ pressure has a quantitatively much stronger effect than $\langle 110\rangle$ pressure. We summarize our $\langle 100\rangle$ pressure data with the phase diagram in Fig. 7. It appears very likely that strong $\langle 100\rangle$ pressure changes the principal axes of the order from $\langle 110\rangle$ to $\langle 100\rangle$, in other words that unstressed $CeAuSb_2$ has a subleading susceptibility to a $\langle 100\rangle$ order which becomes dominant with sufficient applied $(100)/(010)$ orthorhombicity. The simplest example to imagine is that the in-plane propagation vector of the spin-density wave rotates from $(\eta, \pm\eta)$ to $(\eta_2,0)$ or $(0,\eta_2)$, with η_2 in general not equal to η. The first piece of evidence for rotation of the principal axes is the first-order transition at $\varepsilon_{100} \approx -0.5\%$: Electronic orders generally pin to high-symmetry directions of the host lattice, so rotation between $\langle 110\rangle$ and $\langle 100\rangle$ principal axes should, in general, be discontinuous. The second is the strong linear dependence of the transition temperature T_2 on $\langle 100\rangle$ pressure, in other words on applied $(100)/(010)$ orthorhombicity. In principle, the linear dependence could also be due to coupling to unit-cell volume and/or interplane spacing, parameters that also vary linearly with applied $\langle 100\rangle$ pressure. However, unless the mechanical properties of

$CeAuSb_2$ are extraordinarily anisotropic, ⟨110⟩ pressure will yield changes similar to these parameters, and yet it has much less effect on the magnetic transition.

In the density functional theory calculations reported in Ref. [11], nesting vectors parallel to ⟨100⟩ directions as well as ⟨110⟩ directions were found, so $CeAuSb_2$ may well have a strong subleading susceptibility to a ⟨100⟩ spin-density wave. A more complicated textured order such as the field-induced "woven" order proposed in Ref. [11], which has ⟨100⟩ principal axes, is also, in principle, a possibility; however, this order was proposed as a way to accommodate both strong nesting and strong field-induced polarization, and at zero field a straightforward spin-density wave seems generically more likely.

The phase diagrams against ⟨100⟩ and ⟨110⟩ pressure are our main results. In the remainder of this paper we discuss a different topic, the possibility that the Néel transition, for $|\varepsilon_{100}| < 0.25\%$, is driven first-order by competing fluctuations and that uniaxial pressure restores a continuous transition by selecting a preferred direction and eliminating the competition.

We can rule out an alternative explanation for the first-order transition, strong magnetoelastic coupling. If the gain in magnetic condensation energy from a given lattice distortion exceeds its elastic energy cost, then the transition becomes first order [17]. The strain dependence of T_N may be written as $T_N = T_{N,0}(1 + \beta\varepsilon)$, with β being a coupling constant and ε being a strain associated with the mode of deformation most strongly favoring the ordered phase. The heat capacity of a material is $C = -T\frac{\partial^2 F}{\partial T^2}$, where F is the free energy. For T close to and below a second-order transition at T_N, this expression may be integrated:

$$\Delta F = \frac{\Delta C}{2T_N}(T_N - T)^2,$$

where ΔC and ΔF are the change in heat capacity and free energy due to the magnetic order. ΔC, from the data in Fig. 2, is $\sim 1 \times 10^5$ J/m^3 K. The elastic energy cost of lattice deformation is $\Delta F = (E/2)\varepsilon^2$, where E is the elastic modulus associated with strain ε. The elastic compliance drives the transition first-order if the gain in condensation energy exceeds the elastic energy cost, i.e., if $E - \Delta C T_{N,0}\beta^2 < 0$.

Although the elastic moduli of $CeAuSb_2$ have not been measured, we may take $E \sim 100$ GPa, a typical Young's modulus for metals, as an order-of-magnitude estimate. Therefore, a first-order transition is expected if β exceeds $\sim$400. With uniaxial pressure, $dT_N/d\varepsilon$ is not nearly so large: The steepest $\varepsilon \to 0$ strain dependence is obtained with tensile ⟨110⟩ pressure, for which $|dT_N/d\varepsilon| \approx 94$ K, yielding $\beta \approx 14$. We also tested the effect of biaxial pressure, by epoxying thin samples of $CeAuSb_2$ to titanium and aluminum plates and using the differential thermal contraction to apply biaxial pressure. The differential thermal contraction between these materials between room temperature and $T \to 0$ is 0.25%, and the observed difference in T_N was 0.04 K, yielding $\beta \sim 2.5$. This measured value of β might be suppressed by plastic deformation of the epoxy during the initial stages of the cooldown, which would relax some of the thermal stress; however, it is orders of magnitude too low to drive a first-order transition.

Instead, we propose that the transition is driven first-order by fluctuations. The magnetic order in $CeAuSb_2$ persists even if the RRR is below 3 [3], indicating a robust order with a short range of interaction, which favors stronger fluctuation effects [18,19]. Competition between fluctuations in the disordered state can drive a transition first-order; in theoretical studies of magnetic helices in MnSi [20], density wave order in layered cuprates [21,22], and general multicomponent orders [5], a continuous transition is predicted when all possible components of the order can condense simultaneously. However, there is competition in $CeAuSb_2$, where condensation of, e.g., $(\eta, \eta, 1/2)$ prevents condensation of $(\eta, -\eta, 1/2)$ order. Reference [5] provides a more precise criterion for fluctuation-driven first-order transitions. Ordered phases were studied with a fourth-order, multicomponent Ginzburg-Landau Hamiltonian, in which the strength of competition between the components is set by the coefficients of the biquadratic terms [Eq. (2.1) of that paper]. The Hamiltonian was constructed so that either one or all of the components could condense: The coefficients of the biquadratic terms were set equal, and if this coefficient is below a threshold, then the components may coexist in mean-field theory, and if it is above that threshold, condensation of one precludes condensation of all others. It was found that if the number of components n is $\geqslant 4$, a first-order transition is expected as soon as the biquadratic coefficient exceeds this threshold, i.e., as soon as only one component condenses in mean-field theory. (For $n < 4$, stronger competition is required to get a first-order transition.) n is at least 4 in $CeAuSb_2$: There are two possible density-wave orientations, and because they are incommensurate, there are phase and amplitude degrees of freedom for each.

Restoring a continuous transition is predicted to require symmetry-breaking fields exceeding a noninfinitesimal threshold strength [5,6,21]. The clearest experimental demonstration is on the antiferromagnetic transition of MnO. It is first order but becomes continuous under uniaxial stress [23], a result explained through the effect of reduced point-group symmetry on fluctuations [24,25]. However, this demonstration is over 40 years old, and the present piezoelectric-based pressure apparatus offers much better resolution. In $CeAuSb_2$, ⟨100⟩ pressure appears to restore a continuous transition by rotating the principal axes to ⟨100⟩ and selecting a preferred direction between (100) and (010). Strong ⟨110⟩ pressure should also restore a continuous transition by selecting between the (110) and $(1\bar{1}0)$ directions; however, the weak coupling between the electronic system and ⟨110⟩ lattice deformation means that this may occur at a pressure beyond what we were able to apply.

ACKNOWLEDGMENTS

We acknowledge the financial support of the Max Planck Society. J.P. acknowledges the financial support of the National Research Foundation of Korea (NRF) funded by the Ministry of Science and ICT (No. 2016K1A4A4A01922028). H.S. acknowledges the financial support of PRESTO, JST (Grant No. JPMJPR16R2) and a Grant-in-Aid for Young Scientists (Grant No. 16H06015). We thank C. Broholm and E. Berg for useful discussions and P. Canfield and V. Fritsch for their assistance with sample growth.

The raw data for this publication may be downloaded at https://dx.doi.org/10.17617/3.14 or https://edmond.mpdl.mpg.de/imeji/collection/BpfLLXbRBEOTjMHX.

[1] R. M. Fernandes, A. V. Chubukov, J. Knolle, I. Eremin, and J. Schmalian, Phys. Rev. B **85**, 024534 (2012).
[2] F. Kretzschmar, B. Muschler, T. Böhm, A. Baum, R. Hackl, H.-H. Wen, V. Tsurkan, J. Deisenhofer, and A. Loidl, Phys. Rev. Lett. **110**, 187002 (2013).
[3] A. Thamizhavel, T. Takeuchi, T. Okubo, M. Yamada, R. Asai, S. Kirita, A. Galatanu, E. Yamamoto, T. Ebihara, Y. Inada, R. Settai, and Y. Onuki, Phys. Rev. B **68**, 054427 (2003).
[4] L. Balicas, S. Nakatsuji, H. Lee, P. Schlottmann, T. P. Murphy, and Z. Fisk, Phys. Rev. B **72**, 064422 (2005).
[5] E. Domany, D. Mukamel, and M. E. Fisher, Phys. Rev. B **15**, 5432 (1977).
[6] S. J. K. Jensen, O. G. Mouritsen, E. K. Hansen, and P. Bak, Phys. Rev. B **19**, 5886 (1979).
[7] P. C. Canfield and Z. Fisk, Philos. Mag. B **65**, 1117 (1992).
[8] P. C. Canfield and I. R. Fisher, J. Cryst. Growth **225**, 155 (2001).
[9] S. Seo, V. A. Sidorov, H. Lee, D. Jang, Z. Fisk, J. D. Thompson, and T. Park, Phys. Rev. B **85**, 205145 (2012).
[10] L. Zhao, E. A. Yelland, J. A. N. Bruin, I. Sheikin, P. C. Canfield, V. Fritsch, H. Sakai, A. P. Mackenzie, and C. W. Hicks, Phys. Rev. B **93**, 195124 (2016).
[11] G. G. Marcus, D.-J. Kim, J. A. Tutmaher, J. A. Rodriguez-Rivera, J. O. Birk, C. Niedermeyer, H. Lee, Z. Fisk, and C. L. Broholm, arXiv:1707.01611.
[12] C. W. Hicks, M. E. Barber, S. D. Edkins, D. O. Brodsky, and A. P. Mackenzie, Rev. Sci. Instrum. **85**, 065003 (2014).
[13] C. W. Hicks, D. O. Brodsky, E. A. Yelland, A. S. Gibbs, J. A. N. Bruin, M. E. Barber, S. D. Edkins, K. Nishimura, S. Yonezawa, Y. Maeno, and A. P. Mackenzie, Science **344**, 283 (2014).
[14] H.-H. Kuo, M. C. Shapiro, S. C. Riggs, and I. R. Fisher, Phys. Rev. B **88**, 085113 (2013).
[15] D. O. Brodsky, M. E. Barber, J. A. N. Bruin, R. A. Borzi, S. A. Grigera, R. S. Perry, A. P. Mackenzie, and C. W. Hicks, Sci. Adv. **3**, e1501804 (2017).
[16] S. R. Saha, H. Sugawara, T. Namiki, Y. Aoki, and H. Sato, Phys. Rev. B **65**, 214429 (2002).
[17] C. P. Bean and D. S. Rodbell, Phys. Rev. **126**, 104 (1962).
[18] V. L. Ginzburg, Sov. Phys. Solid State **2**, 1824 (1961).
[19] K. Binder, Rep. Prog. Phys. **50**, 783 (1987).
[20] P. Bak and M. H. Jensen, J. Phys. C **13**, L881 (1980).
[21] A. J. Millis, Phys. Rev. B **81**, 035117 (2010).
[22] M. De Prato, A. Pelissetto, and E. Vicari, Phys. Rev. B **74**, 144507 (2006).
[23] D. Bloch, D. Hermann-Ronzaud, C. Vettier, W. B. Yelon, and R. Alben, Phys. Rev. Lett. **35**, 963 (1975).
[24] S. A. Brazovskiĭ and I. E. Dzyaloshinskiĭ, JETP Lett. **21**, 164 (1975).
[25] P. Bak, S. Krinsky, and D. Mukamel, Phys. Rev. Lett. **36**, 829 (1976).